Signal Processing 127 (2016) 227–238

Contents lists available at ScienceDirect

Signal Processing

journal homepage: www.elsevier.com/locate/sigpro

# Correcting CNA phase mismatch phenomena in frequency blind equalization for OFDM systems

Vincent Savaux [a,*], Faouzi Bader [a], Jacques Palicot [a]

[a] SCEE team/IETR, CentraleSupélec, Rennes, France

ARTICLE INFO

*Article history:*
Received 23 July 2015
Received in revised form
17 February 2016
Accepted 26 February 2016
Available online 15 March 2016

*Keywords:*
Blind equalization
Constant norm algorithm
OFDM

ABSTRACT

This paper presents an adaptation of the constant norm algorithm (CNA) class for frequency blind equalization in orthogonal frequency division multiplexing (OFDM) modulation. Originally designed in single-carrier systems, the convergence analysis of CNA is investigated in OFDM. It results that a phase adaptation of the equalizer coefficient has to be undertaken to ensure a convergence toward the expected value, leading to the proposed phase adaptation procedure (PAP). Furthermore, a sub-optimal initialization strategy is proposed, which allows to improve the convergence speed of the algorithm. Simulations show that the proposed CNA with PAP outperforms the constant modulus algorithm (CMA) for both the convergence speed and the steady-state performance. Furthermore, a gain in number of iterations of up to 50% is achieved when the proposed sub-optimal initialization is used compared with a fixed initialization value.

© 2016 Elsevier B.V. All rights reserved.

## 1. Introduction

The robustness of orthogonal frequency division multiplexing with cyclic prefix (CP-OFDM) against multipath channels has made it a very popular modulation scheme that has been adopted in a large number of communication standards. The use of a CP longer than the delay spread of the channel allows us to suppress the inter-symbols interference and recover the orthogonality between subcarriers at the receiver. Furthermore, the remaining channel distortions can be easily estimated by using pilot symbols that are multiplexed in the data stream. Overviews and comparative studies of data-aided channel estimation methods for OFDM systems are provided in [1–3]. Once estimated, the channel can be directly inverted with a one-tap per carrier equalization. However, the use of the CP and pilot symbols may drastically reduce the useful data rate. Therefore, the pilot density reduction or the CP length shortening is recommended for higher data rate transmissions. Such capabilities can be reached, in particular by means of blind equalization.

First works dealing with blind equalization have been undertaken by Sato [4] in 1975, but one of the most used algorithms is the constant modulus algorithm (CMA) proposed by Godard [5] in 1980 (and independently in [6] in 1983), and an overview on blind equalization using CMA is presented by Johnson et al. [7]. The CMA converges independently of the phase, but this feature leads to a misadjustment in the detected symbols, which needs to be corrected. The multimodulus algorithm (MMA) presented in [8] (originally called modified CMA [9,10]) has been proposed to solve the phase ambiguity issue by employing the CMA on both the real and imaginary parts of the received symbols. More recently, MMA-based methods have been derived in order to improve the performance of CMA for high-order constellations [11,12]. In particular, the $\beta$-MMA method such as proposed in [13,14] has proven to outperform both CMA and MMA.

In CP-OFDM systems, the blind equalization is generally carried out for two purposes:

(i) Performing a channel shortening, when the delay spread is longer than the CP duration. In that case, a deconvolution filter is used as time-domain equalizer (TEQ). The equalizer coefficients can then be updated by using some features of the OFDM signal. A solution consists of minimizing the difference between the last samples of the OFDM symbol and the corresponding samples in the CP, as presented in [15]. In [16], the authors propose to use a mean square criterion on the "artificial" null symbols between subcarriers. Another method in [17] aims to maximize the signal to interference plus noise ratio (SINR).

(ii) Performing a simple frequency per-carrier equalization. In [18], the simple decision directed algorithm is used, in which the considered cost function compares the received signal and the detected data after a decoding stage. The authors in [19] have proposed an algorithm based on the maximum

* Corresponding author.
*E-mail addresses:* vincent.savaux@centralesupelec.fr (V. Savaux), Faouzi.Bader@supelec.fr (F. Bader), jacques.palicot@centralesupelec.fr (J. Palicot).

http://dx.doi.org/10.1016/j.sigpro.2016.02.024
0165-1684/© 2016 Elsevier B.V. All rights reserved.

likelihood (ML) criterion. Although this blind equalizer shows good performance, it is particularly complex, especially if numerous subcarriers and high order constellations are considered.

Alternatively, both channel shortening and frequency equalization can be performed by the per-tone equalization method which has been originally proposed in [20], and transposed to blind receivers in [21,22]. In this paper, we rather focus on per-carrier frequency equalization. This task is performed by using the constant norm algorithm (CNA) proposed in [23,24]. This method can be seen as a generalization of the CMA, in which the modulus is substituted by a norm on the complex plane. In this way, a specific norm fits a particular constellation which allows us to reduce the noise of the algorithm. The CNA has been presented for single-carriers systems in [24], and to the best of the authors' knowledge, it has not been used in multicarrier systems. It is worth noting that the special case of the infinity norm has been independently proposed in [24–27], and has been originally called *square contour algorithm* (SQA). One of the main goals of this paper is to extend the CNA to the OFDM context by including specific adaptations. As a matter of fact, the phase mismatch between the channel and the equalizer coefficient has to be taken into account to ensure that the update algorithm converges toward the expected value. Thus, we propose to add a phase adaptation procedure (PAP) to the CNA in order to cancel the phase mismatch phenomenon. Furthermore, a quasi-optimal initialization strategy for each of the equalizer's coefficients is proposed.

The remaining of the paper is organized as follows: Section 2 presents the system model and the used equalization algorithms. The convergence behavior of CNA is analyzed in Section 3, and the proposed phase adaptation procedure is presented in Section 4. Then, a sub-optimal initialization value is provided in Section 5. Simulations will show achieved performances of the CNA with its adaptations to OFDM in Section 6, and we draw our conclusions in Section 7.

## 2. Background

### 2.1. System model

The transmission of OFDM symbols over a multipath channel is considered with a perfect time and frequency synchronization. It is assumed that the cyclic prefix (CP) duration is longer than the maximum delay spread of the channel. Therefore, after the fast Fourier transform (FFT) of size $M$ and the CP removal, the $n$th received OFDM signal is expressed as

$$\mathbf{Y}_n = \mathbf{H}_n\mathbf{X}_n + \mathbf{W}_n, \tag{1}$$

where $\mathbf{X}_n$ and $\mathbf{Y}_n$ are the $M \times 1$ vectors containing the transmitted and received complex symbols $Y_{m,n}$ and $X_{m,n}$ respectively, and the $m$ subscript is pointing out the subcarrier index. The vector $\mathbf{W}_n$ is composed of $M$ independent zero-mean Gaussian noise samples whose variance is $\sigma^2$, and $\mathbf{H}_n$ is the $M \times M$ diagonal matrix of the channel with entries

$$H_{m,n} = H_m = \sum_{l=0}^{L-1} h_l e^{-2j\pi\frac{m\tau_l}{M}}, \tag{2}$$

on the diagonal. The removal of the subscript $n$ in (2) means that the channel is assumed to be static throughout the paper. The constant $L$ in (2) is the number of paths of the channel, $h_l$ is the path gain, and $\tau_l$ is the corresponding delay. More details related to the derivation of (1) and (2) are provided in Chapter 1 of [28].

### 2.2. Blind equalization: problem formulation

The equalization aims at recovering the transmitted data $\mathbf{X}_n$ from the received signal $\mathbf{Y}_n$. The equalization in OFDM systems can be undertaken on each subcarrier independently of each other by the following expression:

$$Z_{m,n} = F_{m,n}Y_{m,n} = F_{m,n}(H_{m,n}X_{m,n} + W_{m,n}), \tag{3}$$

where $F_{m,n}$ is the equalizer coefficient on the $m$th subcarrier. In this paper, the coefficients $F_{m,n}$ are blindly adapted by solving the following optimization problem:

$$F_m^{opt} = \min_{F_m}(E\{J(Z_m)\}), \tag{4}$$

where $E\{\cdot\}$ is the mathematical expectation, and $J$ is a given cost function that will be determined afterward. The minimization problem in (4) can be carried out by employing the classical stochastic gradient algorithm as

$$F_{m,n+1} = F_{m,n} - \mu\frac{\partial J(Z_{m,n})}{\partial Z_{m,n}}, \tag{5}$$

where $\mu$ is the appropriate step-size parameter. Since the cost function $J$ may be phase-blind, the demodulation stage in (1) and the convergence process in (5) may lead to a phase error $\phi_{m,n}$. As a consequence, a phase recovery and tracking algorithm must be added to the equalizer in order to track both the phase and the modulus of the transmitted symbols [5,29,10], such as depicted in Fig. 1, and expressed as

$$\phi_{m,n+1} = \phi_{m,n} - \mu_\phi f(\tilde{Z}_{m,n}), \tag{6}$$

where $\mu_\phi$ is the step size parameter for the phase tracking algorithm, and $f$ is a given function. The simple decision directed has been used in [5] for the phase tracking, but this method is limited when the variation speed of the phase is to high. Some more recent techniques have been proposed in the literature in order to overcome this problem, such as in [30,31]. However, it has been aforementioned that the symbols $Y_{m,n}$ are received with perfect synchronization, and the channel is supposed to be static. Therefore, the phase tracking is out of the scope of this paper, and we focus on the way to perform (5) in the following.

### 2.3. Constant norm algorithm

As a general rule, the cost function $J$ in (5) compares the output of the equalizer $Z_{m,n}$ with a constant value. One of the most frequently used cost function is the CMA presented by Godard [5]. CMA is particularly adapted for constant modulus constellations as phase shift keying (PSK), but also works for square constellation as QAM. A generalization of this function called CNA has been proposed in [24]. The authors have shown that CNA fits better QAM constellations than CMA, as a particular norm can be adapted for each modulation. As presented in [24], the cost function of CNA can be written as

$$J(Z_m) = \frac{1}{ab}\,||Z_m||^a - R|^b, \tag{7}$$

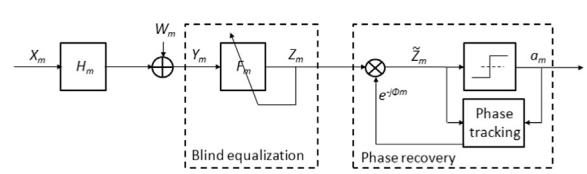


**Fig. 1.** Blind equalization and phase recovering process on each subcarrier $m$ at the OFDM receiver.

دانلود کننده مقالات علمی freepaper.me FREE paper

where $\|\cdot\|$ is a norm defined on $\mathbb{C}$, $R$ is a real positive constant that depends on the constellation type, and $a$ and $b$ are two parameters that give two degrees of freedom to the algorithm. However, the most frequently used values are $a = b = 2$[1] and will be considered throughout the present paper. It has been demonstrated in [5,24] that the optimal value $\alpha_m = |F_m H_m| = 1$ should be reached if

$$R = \frac{E\{\| X_m \|^{2a}\}}{E\{\| X_m \|^{a}\}}. \tag{8}$$

We can consider (8) as the most general expression of $R$, which is valid for any norm, and whose derivation is provided by (9)–(14) in [24]. In the rest of the paper, we consider the $p$-norm family, which is expressed for any complex $z$ on the plane $\mathbb{C}$ as

$$\| z \|_p = \sqrt[p]{|\mathrm{Re}\{z\}|^p + |\mathrm{Im}\{z\}|^p}. \tag{9}$$

The CMA is obtained by considering $p=2$, i.e. the "usual norm". In that case, the update algorithm in (5) can be rewritten as follows:

$$F_{m,n+1} = F_{m,n} - \mu(|Z_{m,n}|^2 - R)Z_{m,n}Y^*_{m,n}. \tag{10}$$

Thus, CMA is a particular case of the more general CNA family. In [24], the cases $p=6$ and $p = \infty$ have also been studied as they are relevant for QAM constellations (especially 16-QAM). Since we focus our developed analysis on the square 16-QAM constellation, we will consider these two norms in the rest of the paper.[2] Note that the update algorithms related to CNA-6 and CNA $-\infty$ are

$$F_{m,n+1} = F_{m,n} - \mu(\| Z_{m,n} \|_6^2 - R) \times \frac{\mathrm{Re}\{Z_{m,n}\}^5 + j\,\mathrm{Im}\{Z_{m,n}\}^5}{\| Z_{m,n} \|_6^4} Y^*_{m,n}, \tag{11}$$

and

$$F_{m,n+1} = F_{m,n} - \mu(\| Z_{m,n} \|_\infty^2 - R) f(Z_{m,n}) Y^*_{m,n}, \tag{12}$$

where the infinite norm is $\| Z_{m,n} \|_\infty = \max(|\mathrm{Re}\{Z_{m,n}\}|, |\mathrm{Im}\{Z_{m,n}\}|)$ and $f$ is a function defined as

$$f(Z_{m,n}) = \begin{cases} \mathrm{Re}\{Z_{m,n}\}, & \text{if } |\mathrm{Re}\{Z_{m,n}\}| > |\mathrm{Im}\{Z_{m,n}\}| \\ j\,\mathrm{Im}\{Z_{m,n}\}, & \text{otherwise} \end{cases}. \tag{13}$$

As it was highlighted in [23,24], the infinite norm does not belong to the $p$-norm family, and the derivation of (12) requires specific developments. Besides, the unit ball of the infinite norm is a square of side 2, therefore the authors of [23,24] named the update algorithm in (12) Constant sQuare Algorithm (CQA). It is worth noting that the output of the equalizer is constrained by the unit ball of the utilized norm. For instance, the equalized symbols $Z_{m,n}$ are on a circle when CNA-2 (CMA) is used, whereas they are on a square if CQA is chosen.[3] Fig. 2 depicts the unit balls of the modulus and the infinite norms compared with the symbols of a 16-QAM. Since the steady-state performance of the algorithm depends on the mean distance $E\{l\}$ between the constellation symbols and the unit ball (see Section 2 in [23] for more details), it can be easily shown that $E\{l_\infty\} < E\{l_2\}$. In fact, if it is supposed that the circle in Fig. 2 has a radius of 1, then we obtain:

$$E\{l_\infty\} = \frac{4 \times 1 + 12 \times 0}{16} = 0.25$$

$$E\{l_2\} = \frac{8 \times 0.0541 + 4 \times 0.5286 + 4 \times 0.4142}{16} = 0.2627,$$

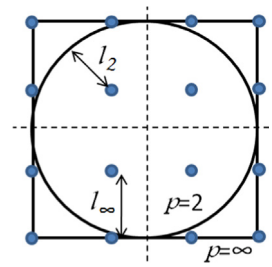


**Fig. 2.** Distance between the unit balls corresponding to CMA (circle) and CNA $-\infty$ (square), and the symbols of the 16-QAM constellation.

where 0.0541, 0.5286, and 0.4142 correspond to the distances between the points $\{\pm\frac{1}{3} \pm j, \pm 1 \pm \frac{1}{3}j\}$, $\{\pm\frac{1}{3} \pm \frac{1}{3}j\}$, and $\{\pm 1 \pm j\}$ respectively, and the unit circle. Thus, the performance of the CNA $-\infty$ should be better than that of CMA using a 16-QAM constellation. This will be further explained and shown through simulations in Section 6.

As previously mentioned, the CNA has been proposed for single carrier systems where the blind equalization is a blind deconvolution [24]. To the best of the authors' knowledge, this concept has not been adapted and used in OFDM systems, which is the main purpose of this paper.

## 3. Convergence analysis of CNA in OFDM

One of the advantages of the CMA is its phase-independence nature as demonstrated in [5,7]. This can be straightforwardly shown by substituting $Z_{m,n} = F_{m,n}Y_{m,n}$ into (10), which yields the following expression:

$$F_{m,n+1} = F_{m,n}(1 - \mu(|Z_{m,n}|^2 - R)|Y_{m,n}|^2). \tag{14}$$

It can be noticed that $(1 - \mu(|Z_{m,n}|^2 - R)|Y_{m,n}|^2)$ (14) is real. It results that the phase of $F_{m,n}$ is that used at the initialization $F_{m,n=0}$. Geometrically, the CMA can be interpreted as a projection of the received symbols $Y_{m,n}$ on a given circle as shown in Fig. 2. As a consequence, the direction of $F_{m,n}$ is not a limiting parameter for the convergence of CMA.

It has been stated in [23,24] that the CNA is able to recover the phase in single carrier systems. However, this is obtained to the cost of an additive delay in the convergence process compared with CMA. Such a result is valid for a blind deconvolution in single carrier systems but might be reconsidered in the present OFDM context where the equalization is performed by a single coefficient per carrier as in (11) and (12). In particular, it can be noticed for CQA that

$$E\{\arg(F_{m,n+1})\} = E\{\arg(F_{m,n})\} = E\{\arg(F_{m,n=0})\}. \tag{15}$$

The difference between the result in (14) and (15) is that CMA converges in the same direction as $F_{m,n=0}$ in a deterministic way (it is a projection), whereas CQA converges "in average" in the direction of $F_{m,n=0}$. The equality in (15) is proved in Appendix A. The unit ball of CMA is a circle, so the phase of $F_{m,n}$ does affect its modulus when the steady-state is reached. On the other hand the unit ball of CQA is a square, therefore the convergence of $F_{m,n}$ in the direction of the side or the corner of the square shall not lead to the same results, reflecting that the convergence of CQA depends on the phase of $F_{m,n=0}$ as shown in (15).

Besides the previous geometrical considerations, it is possible to mathematically show that the result $|F_m^{opt}H_m| = \alpha_m = 1$, which is verified for any $F_{m,0}$ value using CMA, is not ensured anymore for CQA. To achieve this, the optimization problem in (4) is solved by

[1] It has been stated in [5] that it is very difficult to ensure the convergence of the algorithm for $a$ and $b$ values higher than 2.

[2] More generally, it has been shown by the authors of [24] that for any constellation corresponds a specific norm.

[3] The equalities $\| Z_{m,n} \|^2 - R = 0$ and $\| Z_{m,n} \|_\infty^2 - R = 0$ are achieved in (10) and (12) if the steady state is reached, and correspond to the equations of the circle and the square on the complex plane, respectively.

دانلود کننده مقالات علمی freepaper.me FREE paper

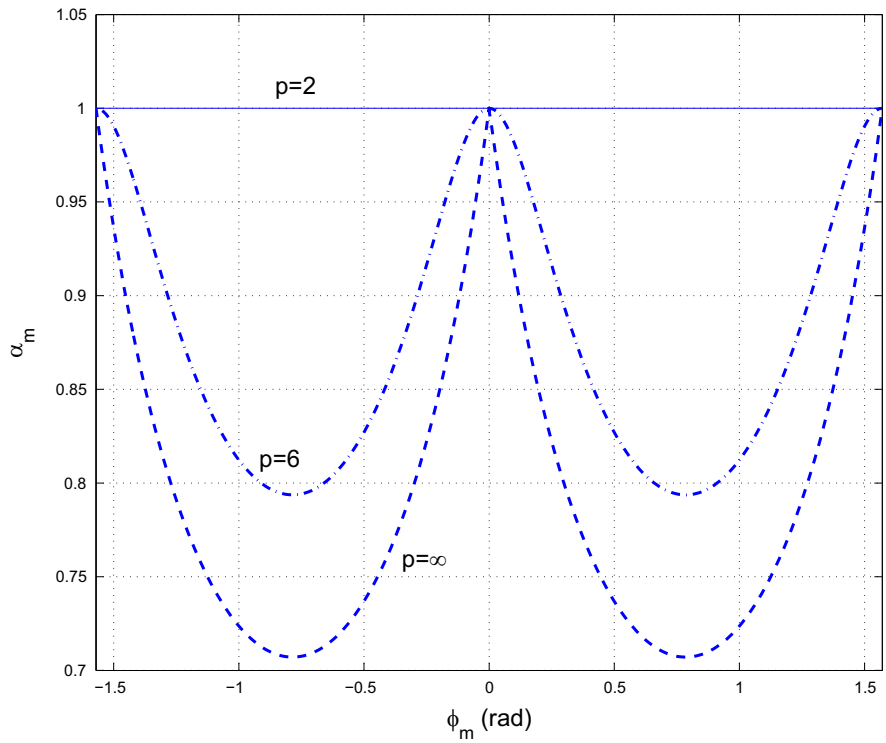


**Fig. 3.** Achieved $\alpha_m$ in (17) versus phase mismatch $\phi_m$ for $p=2$, $p=6$, and $p=\infty$.

assuming (i) a noiseless transmission, (ii) the optimal value $F_m^{opt}$ is reached with a phase mismatch $\phi_m$ with the channel such as $F_m^{opt}H_m = \alpha_m^{opt}e^{j\phi_m}$ (i.e. $\phi_m$ is the angle between $F_m$ and $H_m$) and (iii) $R$ is defined as in (8). For sake of simplicity, further developments are carried out considering that $a = b = 2$. The optimal value $\alpha_m^{opt}$ is obtained by solving the following expression:

$$\left.\frac{\partial E\{J(Z_m)\}}{\partial \alpha_m}\right|_{\alpha_m=\alpha_m^{opt}} = 0. \tag{16}$$

The optimization problem is rewritten by substituting (7) into (16) leading to

$$\begin{aligned}\left.\frac{\partial E\left\{\frac{1}{4}\,\|Z_m\|^2 - R\right|^2\}}{\partial \alpha_m}\right|_{\alpha_m=\alpha_m^{opt}} &= 0 \Leftrightarrow E\{\alpha_m^3 \,\|\, e^{j\phi_m}X_m \,\|^2\} \\ &= E\{\alpha_m R \,\|\, e^{j\phi_m}X_m \,\|\} \Leftrightarrow \alpha_m \\ &= \left(\frac{R\cdot E\{\|\, e^{j\phi_m}X_m \,\|^2\}}{E\{\|\, e^{j\phi_m}X_m \,\|^4\}}\right)^{\frac{1}{2}}.\end{aligned} \tag{17}$$

Fig. 3 depicts achieved $\alpha_m$ versus $\phi_m$ from $-\frac{\pi}{2}$ to $\frac{\pi}{2}$ for $p=2$, $p=6$, and $p=\infty$. The used constellation is a 4-QAM. Fig. 3 confirms that CMA (i.e. CNA with $p=2$) converges to the optimal value $\alpha_m = 1$ whatever the phase $\phi_m$ is. However, it can be observed that the phase mismatch ($\phi_m \neq 0$) for $p=6$ and $p=\infty$ will conduct to a non-optimal value $\alpha_m \neq 1$. In particular, it can be observed for $p=\infty$ that at $\phi_m = \pm\frac{\pi}{4}$ we have $\alpha_m = 1/\sqrt{2}$, which corresponds to the length of half the diagonal of a square of side 2. The phase mismatch $\phi_{m,n}$ has no incidence if $p=2$ since the unit ball is a circle, but induces an increase of $1/\alpha_m$ if $p > 2$. Fig. 4 illustrates this phenomenon for CQA (for which the unit ball is a square) using $\arg(F_{m,n=0}) = 0$, and $\phi_m < 0$. Thus, $|F_{m,n}|$ converges to $\frac{\alpha_m}{|H_{m,n}|}$ with $\alpha_m \leq 1$.

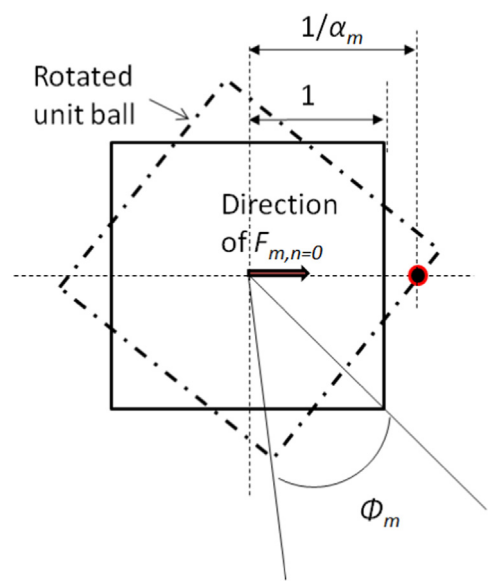


**Fig. 4.** Geometrical interpretation of the effect of the phase rotation $\phi_m$ on $\alpha_m$, using $p=\infty$.

It has been proved in (15) that CQA converges in the same direction as $F_{m,n=0}$, whereas the phase mismatch between $F_{m,n}$ and $H_{m,n}$ leads to an erroneous $F_{m,n}$ value. Therefore, the convergence of $F_{m,n}$ to non-optimal values such as $\alpha_m \leq 1$ seems to be an inherent property of CQA in OFDM, whereas as aforementioned, the sole effect of the phase mismatch in single carrier systems as in [24] seems to be a delay in the convergence process, in comparison with CMA. In order to overcome this problem, the coefficients $F_{m,n}$ should be chosen with a phase mismatch $\phi_m = 0$. A solution allowing to achieve this result is proposed in Section 4.

freepaper.me FREE paper

## 4. CNA in OFDM with phase adaptation procedure

### 4.1. Basic principle of the phase adaptation procedure

In this section, we propose a procedure for the phase adaptation of the coefficients $F_{m,n}$ allowing to obtain $\phi_m = 0$, and therefore $\alpha_m = 1$. Although the problem of convergence due to the phase mismatch has been shown for the particular case $p = \infty$, the proposed algorithm remains valid whatever the degree $p$ of CNA is. In fact, simulation results in Section 6 show that CNA-6 is able to cancel the phase mismatch in OFDM (with an increase of the convergence delay), whereas the phase mismatch is persistent for CQA. As a consequence, a method that adapts the phase of $F_{m,n}$ according to that of $H_{m,n}$ should be mandatory for CQA, while it shall reduce the convergence time of CNA when $p \neq \infty$. Since the phase adaptation can be used for any $p$ value, we adopt the general formulation "CNA" throughout the section.

The basic idea behind the proposed phase adaptation procedure (PAP)[4] is to re-inject, at a given iteration, the result of the phase recovery $\phi_{m,n}$ in the equalizer coefficient value $F_{m,n}$ instead of the equalized symbol $Z_{m,n}$. This can be viewed as a reset of the equalizer coefficient by replacing $F_{m,n}$ by $F_{m,n}e^{j\phi_{m,n}}$. It must be emphasized that this phase adaptation is relevant only when $\phi_{m,n}$ has converged. This issue is discussed afterward. The steps of the proposed PAP are summarized as follows, and illustrated in Fig. 5.

- If $\phi_{m,n}$ has converged, then
  (a) $F_{m,n} \leftarrow F_{m,n}e^{j\phi_{m,n}}$;
  (b) $\phi_{m,n} \leftarrow 0$;
- else, the iterative blind equalization continues as usual.

### 4.2. Decision rule for performing the PAP

We propose three decision rules for the implementation of the PAP:

1. Decision rule 1 (DR1): An iteration number $n_{PAP}$ is a priori fixed such as if $n = n_{PAP}$, then the PAP is performed. This rule is very simple to implement, but either the PAP is carried out too early and the convergence of $\phi_{m,n}$ is not certainly achieved, or the phase is adapted too late which could affect the convergence speed of the blind equalizer. In order to ensure an optimal value of $n_{PAP}$, the convergence behavior of $\phi_{m,n}$ should be a priori known, but this is not available in practice. However, this solution can be used as a point of comparison for other methods.
2. Decision rule 2 (DR2): This rule consists of comparing a threshold $\gamma_\phi$ with the mean square error (MSE) defined by
$$MSE_{phi,n} = \frac{1}{M}\sum_{m=0}^{M-1} |\phi_{m,n} - \phi_{m,n-1}|^2. \tag{18}$$
The decision rule using $MSE_{phi,n}$ is defined as follows: the threshold $\gamma_\phi > 0$ is set such as if $MSE_{phi,n} < \gamma_\phi$, then the PAP is performed.
3. Decision rule 3 (DR3): Instead of using the MSE in (18), the decision is made independently on each subcarrier $m \in \{0, 1, .., M-1\}$ by using a "local" error
$$\Delta_{m,n}^{phi} = |\phi_{m,n} - \phi_{m,n-1}|^2. \tag{19}$$
Therefore, the PAP is carried out on the $m$th subcarrier if $\Delta_{m,n}^{phi} < \gamma_\phi$. It must be noticed that the threshold $\gamma_\phi$ is the same for DR2 and DR3 as DR2 is only the averaged version of DR3.

[4] Note that we have called the proposed method "phase adaptation procedure" in order to avoid any confusion with the phase tracking algorithm given in (6).

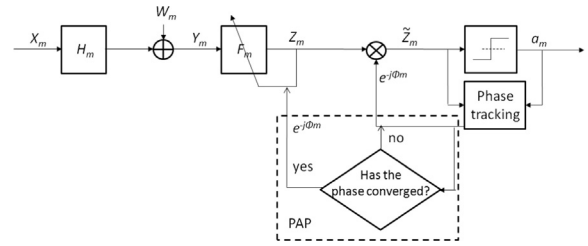


**Fig. 5.** Receiver structure with blind equalization, phase recovering, and phase adaptation procedure (PAP).

Compared with DR2, DR3 takes into account the different convergence speeds of the phases $\phi_{m,n}$, but the variance of the processes $\Delta_{m,n}^{phi}$ is also larger than that of $MSE_{phi,n}$, which could induce erroneous decisions.

The choice of a convenient value of $\gamma_\phi$ is discussed hereafter. The optimal value $\gamma_\phi^{opt}$ can be expressed when the phase $\phi_{m,n}$ has converged by the following expression:

$$\gamma_\phi^{opt} = E\{|\phi_{m,n} - \phi_{m,n-1}|^2 = \mu_\phi^2 E\{\mathrm{Im}\{\tilde{Z}_{m,n}(\tilde{Z}_{m,n} - a_{m,n})^*\}^2\}. \tag{20}$$

As previously mentioned, the optimal value $\gamma_\phi^{opt}$ remains the same for both DR2 and DR3, since the average in (18) is only an approximation of the expectation in (20). Due to the convergence behavior of CQA described in Fig. 4, it would be very difficult to obtain an exact expression of $\gamma_\phi^{opt}$ in (20). However, thanks to some approximations, a minimum value of $\gamma_\phi$ can be derived. To achieve this, we rewrite $\tilde{Z}_{m,n} = Z_{m,n}e^{-j\phi_{m,n}}$ and we obtain the following expression:

$$\begin{aligned}\tilde{Z}_{m,n} &= \underbrace{F_{m,n}e^{-j\phi_{m,n}}H_{m,n}X_{m,n}}_{a_{m,n}+\epsilon_{m,n}} + F_{m,n}e^{-j\phi_{m,n}}W_{m,n} \\ &= a_{m,n} + \underbrace{\epsilon_{m,n} + F_{m,n}W_{m,n}}_{\tilde{W}_{m,n}},\end{aligned} \tag{21}$$

where $\epsilon_{m,n}$ is the error between the equalized symbol and the closest constellation element, and $\tilde{W}_{m,n}$ is equivalent to a noise sample with zero-mean and with variance $\tilde{\sigma}^2$. Due to the presence of $\epsilon_{m,n}$ and $F_{m,n}$ in the expression of $\tilde{\sigma}^2$, it can be assumed that $\tilde{\sigma}^2 \geq \sigma^2$. Therefore, a straightforward development by substituting (21) into (20) yields (more details are in A.1)

$$\gamma_\phi = \mu_\phi^2 E\{\mathrm{Im}\{\tilde{Z}_{m,n}\tilde{W}_{m,n}^*\}^2\} \geq \mu_\phi^2\sigma^2 E\{\mathrm{Re}\{a_{m,n}\}^2 + \mathrm{Im}\{a_{m,n}\}^2\}, \tag{22}$$

where $E\{\mathrm{Re}\{a_{m,n}\}^2 + \mathrm{Im}\{a_{m,n}\}^2\} = 2$ in the case of a 4-QAM, and equal to 10 if a 16-QAM is used. Thus, (22) shows that the chosen value of $\gamma_\phi$ depends on the noise level and the constellation size.

## 5. Sub-optimal initialization strategy

When the blind equalization is carried out with a deconvolution filter in time domain for single carrier systems as in [24], the initialized equalizer consists of a vector composed of zeros except for a unique coefficient that is set to one. In the same ways for OFDM modulations, the initialization strategy consists of setting a unique value $F_{m,n=0}$ for all $0 \leq m \leq M-1$, e.g. $F_{m,n=0} = 1$. However, such an initialization is not optimal with regard to the convergence speed toward the steady-state.

Actually, it is possible to take advantage of the OFDM feature to assess a (sub-)optimal initialization coefficient $F_{m,n=0}^{opt}$ for each subcarrier. For sake of clarity, it is assumed that $n=0$ in the

FREE paper freepaper.me دانلود کننده مقالات علمی

hereafter expressions. The optimal initialization value in the sense of the mean square error criterion can be calculated by minimizing the following cost function:

$$J_m^{ini} = E\{|F_{m,0}Y_{m,0} - X_{m,0}|^2\}. \tag{23}$$

After some straightforward mathematical developments, solving $\frac{\partial J_m^{ini}}{\partial F_{m,0}} = 0$ (i.e. finding the MMSE) leads to

$$F_{m,0}^{opt} = \frac{H_{m,0}^* E\{|X_{m,0}|^2\}}{E\{|Y_{m,0}|^2\}}. \tag{24}$$

One should notice that the equality $E\{|Y_{m,0}|^2\} = |H_{m,0}|^2 E\{|X_{m,0}|^2\}$ holds in noise-free conditions, and hence (24) reduces to $F_{m,0}^{opt} = \frac{1}{H_{m,0}}$. However, it must be emphasized that the value of $H_{m,0}$ is unknown, and the evaluation of $E\{|Y_{m,0}|^2\}$ in (24) requires the prior knowledge of the noise variance, when this is not supposed to be null. Therefore, the optimal initialization coefficient in (24) cannot be assessed in practice. However, a sub-optimal value $F_{m,0}^{s-opt}$ can be derived from (24) by constraining $F_{m,0}^{s-opt} \propto \frac{1}{|H_{m,0}|}$ instead of $F_{m,0}^{opt} = \frac{1}{H_{m,0}}$ when the noise level tends to zero. This feature can be achieved by defining

$$F_{m,0}^{s-opt} = \sqrt{\frac{E\{|X_{m,0}|^2\}}{|Y_{m,0}|^2 + \kappa}}, \tag{25}$$

where $\kappa$ is a real-valued positive constant that avoids the divergence of $F_{m,0}^{s-opt}$ when $Y_{m,0}$ is very close to zero. In practice, it is chosen such that $\kappa \ll 1$. The sub-optimal nature of $F_{m,0}^{s-opt}$ is proved hereafter. The mean error between the square moduli of the invert of $F_{m,0}^{s-opt}$ and $H_{m,0}$ is defined as

$$\epsilon_F = E\left\{\frac{1}{|F_{m,0}^{s-opt}|^2} - |H_{m,0}|^2\right\}. \tag{26}$$

It must be reminded that the noise samples $W_{m,0}$ are zero-mean, have a variance $\sigma^2 = E\{|W_{m,0}|^2\}$, and are uncorrelated with $H_{m,0}$ and $X_{m,0}$ samples. Therefore, the $\epsilon_F$ value in (26) can be simplified as

$$\begin{aligned}\epsilon_F &= E\left\{\frac{|Y_{m,0}|^2 + \kappa}{E\{|X_{m,0}|^2\}} - |H_{m,0}|^2\right\} \\ &= E\left\{\frac{|H_{m,0}X_{m,0}|^2 + |W_{m,0}|^2 + (H_{m,0}X_{m,0})W_{m,0}^*}{E\{|X_{m,0}|^2\}}\right. \\ &\quad \left. + \frac{(H_{m,0}X_{m,0})^* W_{m,0} + \kappa}{E\{|X_{m,0}|^2\}} - |H_{m,0}|^2\right\} = \frac{\sigma^2 + \kappa}{E\{|X_{m,0}|^2\}}.\end{aligned} \tag{27}$$

It can be noticed in (27) that we asymptotically obtain

$$\epsilon_F = \frac{\kappa}{E\{|X_{m,0}|^2\}} \ll 1 \tag{28}$$

when $\sigma^2$ tends to 0 (i.e. when the signal-to-noise ratio tends to infinity). Therefore, the initialization strategy proposed in (25) is sub-optimal, which should improve the convergence speed compared with $F_{m,0=0} = 1$. This behavior will be numerically verified in the hereafter Section 6.

## 6. Simulations results

### 6.1. Simulations setup

The numerical results presented in this section use the following parameters. The OFDM signal is composed of $M = 128$ subcarriers and CP duration is 10% of the OFDM symbol time length. Whatever the chosen algorithm is, the equalizer coefficients are initialized at $F_{m,n} = 1$, and the step-size parameter for the phase is set to $\mu_\phi = 0.1$. Simulations are carried out with a 16-QAM modulation since the used CQA is especially designed to fit this modulation. Furthermore, a SNR of 30 dB is considered in order to compare the limit of the methods, independently of the added noise distortions. The Proakis' channel [32] (refereed as "Proakis 1") whose path coefficients are given by the vector [0.04, − 0.05, 0.07, − 0.21, − 0.5, 0.72, 0.36, 0, 0.21, 0.03, 0.07] is used for simulations. The length of the channel is 86% that of the CP, which guarantees a transmission without intersymbol interference.

The blind equalization algorithms have been compared with the data-aided least square (LS) channel estimation method. In that case, the channel is estimated thanks to a preamble composed of $M$ pilot tones. The power of the preamble has been set equal to the signal. The LS channel estimate is given by

$$H_{m,n}^{LS} = \frac{Y_{m,n}}{X_{m,n}} = H_{m,n} + \frac{W_{m,n}}{X_{m,n}}, \tag{29}$$

where $X_{m,n}$ in (29) is a pilot, whose value is known from the receiver. The channel is then inverted by using the zero forcing equalizer (ZF), whose coefficients are $F_{m,n} = \frac{1}{H_{m,n}^{LS}}$. More details relative to channel estimation is provided in [28]. Furthermore, CMA and CNA are compared with the blind $\beta$-MMA equalizer, the update algorithm of which is detailed in (17) in [13].

The analyzed methods (CMA, CNA, $\beta$-MMA, and LS) are compared by using the following MSE:

$$MSE = \frac{1}{M}\sum_{m=0}^{M-1} (|\tilde{Z}_{m,n}| - |X_{m,n}|)^2. \tag{30}$$

This measure allows us to compare performed algorithms in terms of their converge speeds as well as their steady-state performances. It has been stated in [5] that the optimal step-size parameter should be chosen as $\mu = (30E\{|X_{m,n}|^2\})^{-1}$. However, three blind algorithms (CMA, CNA-6, and CQA) are compared in this paper, and each of them has a different behavior (in terms of convergence speed and/or of steady state performance) for a given $\mu$ value. As a consequence, it should be more relevant to adjust the step-size parameter of each of the methods in order to obtain same convergence speed (and then compare the steady state MSE values), or on the other hand, to compare the convergence speed given the same steady-state performance. In the following, all the plotted results have been obtained after an average over 100 realizations.

### 6.2. Numerical results

Fig. 6 compares the steady-state performance of CMA, CNA-6 and CQA when carried out without PAP, and $\beta$-MMA. To be fair, the compared algorithms start with the same convergence speed, therefore the step-size parameter $\mu$ has been specifically set for each of them. It can be seen that the CQA achieves an MSE steady-state performance equal to −9.5 dB whereas the CMA reaches −17.5 dB. This result is consistent with the analysis undertaken in Section 3. Furthermore, algorithm behaviors in Fig. 6 show that CMA converges faster than CNA-6, but the latter has a lower steady-state than CMA (and has a weaker MSE for $n \geq 4000$ iterations). This proves that CNA-6, unlike CQA, does not require any phase adaptation to converge toward the optimum, but the phase recovering delays the convergence. Furthermore, it can be observed that the $\beta$-MMA achieves the lowest steady-state MSE, but to the cost of a longer delay of convergence. This result is consistent with those that are shown in [13].

FREE paper freepaper.me دانلود کننده مقالات علمی

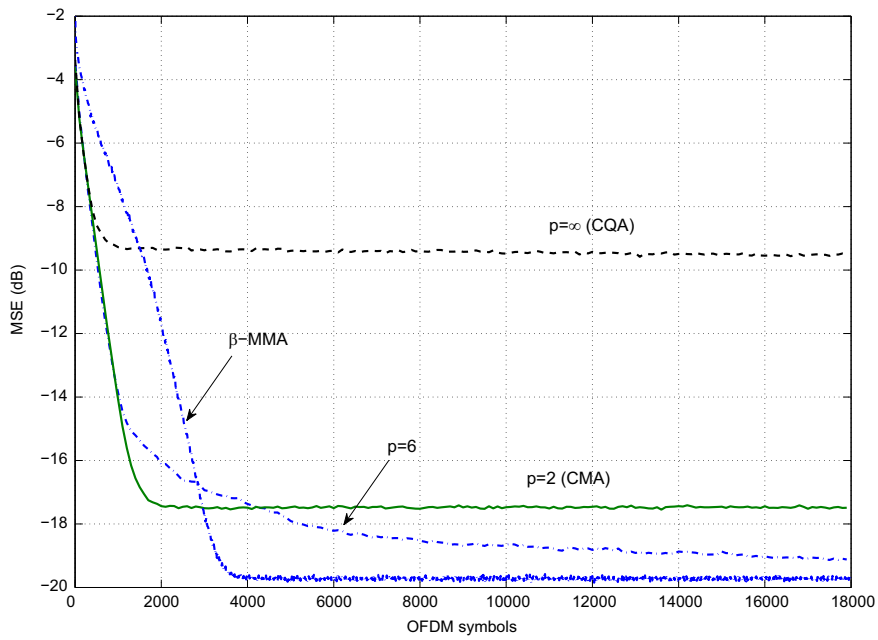


**Fig. 6.** CMA, CNA-6, $\beta$-MMA, and CQA performances versus OFDM symbols numbers on Proakis 1 channel, without PAP.

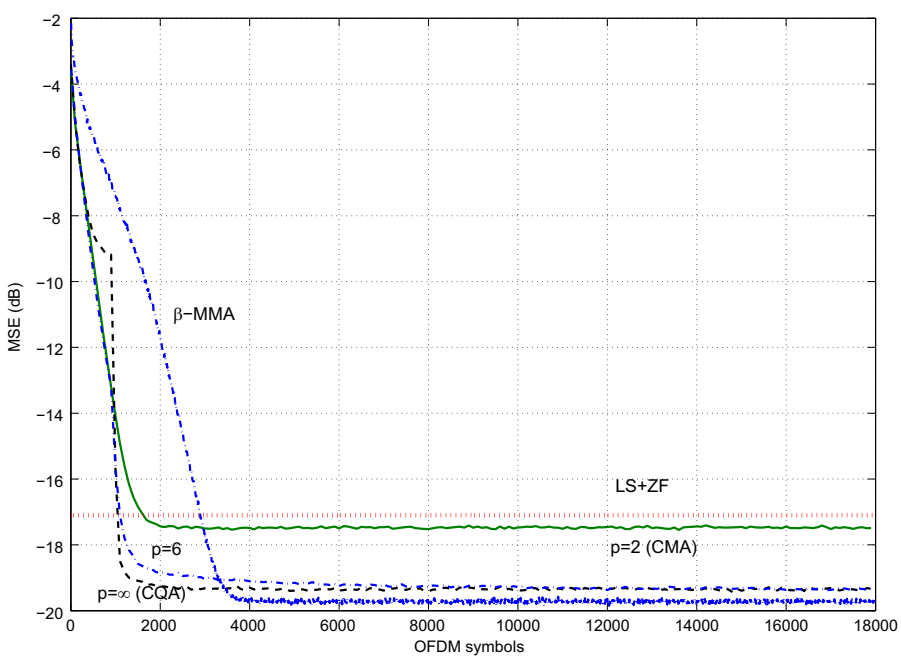


**Fig. 7.** CMA, CNA-6, $\beta$-MMA, and CQA performances versus OFDM symbol numbers on Proakis 1 channel, with PAP using DR1. Comparison with data-aided LS+ZF equalization.

The same parameters as in Fig. 6 are used to compare the MSE performance of CMA, $\beta$-MMA, CNA-6 and CQA with proposed PAP using DR1 with $n_{PAP} = 1000$ (this value has been *a posteriori* set using results from Fig. 9) in Fig. 7. Furthermore, the achieved MSE of LS estimation in (29) with ZF equalization is plotted as well. It can be observed that CNA-6 and CQA have the same steady-state performance at $-19.5$ dB, and CQA has a slightly higher convergence speed than CNA-6. Furthermore, Fig. 7 shows that CNA-6 and CQA achieve higher convergence rate and lower MSE than CMA. It proves that the PAP proposed in Section 4 allows the CQA to be adapted in OFDM systems to achieve similar performances as those observed for single carrier systems in [24,23]. Moreover, although CNA-6 has the same steady-state performance with or without phase adaptation, we draw from Fig. 7 that the PAP increases the convergence speed of the algorithm. The comparison with the pilot-aided LS+ZF method reveals that several hundreds of iterations are required by the blind algorithm to reach the same MSE as LS+ZF, since the latter achieves its steady-state from the first OFDM symbol. However, this drawback is compensated by the fact that a MSE gain of 2.5 is achieved by CNA-6 and CQA in comparison with the data-aided method. Furthermore, the gain of $\beta$-MMA is about 0.5 dB compared with the CNA methods, but it requires 2000 more iteration than CNA to converge. Thus, the performance gain is low in comparison to the additional delay. In addition to the above, the blind methods allows to maximize the spectral efficiency of the signal, since no pilots are used.

Unlike previous figures, Fig. 8 shows the convergence speed of CMA, $\beta$-MMA, CNA-6 and CQA with PAP using DR1 ($n_{PAP} = 1000$)

freepaper.me FREE paper

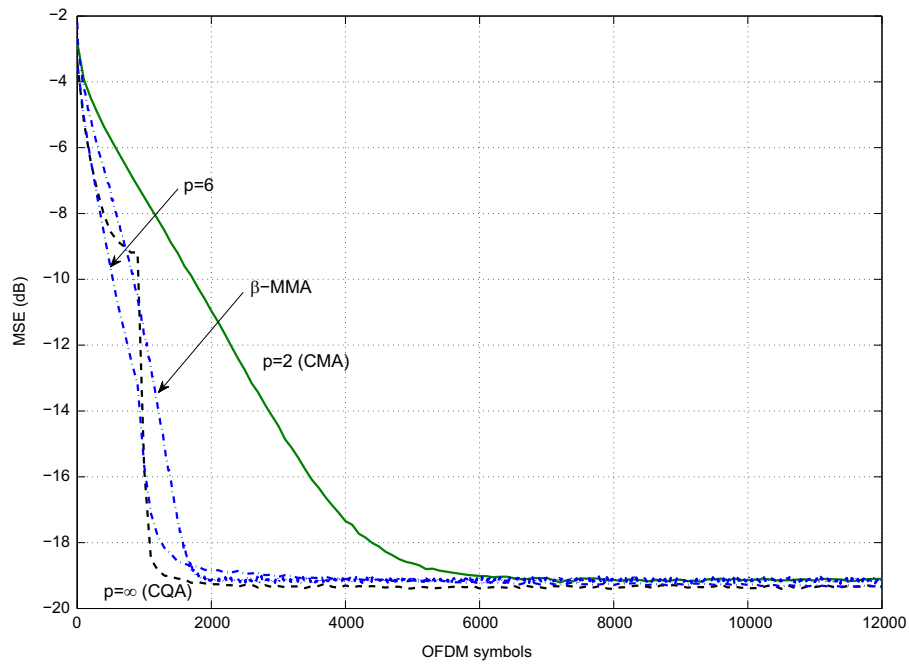


**Fig. 8.** Convergence speed of CMA, CNA-6, $\beta$-MMA, and CQA with PAP using DR1 for a given steady-state performance.

for the same steady state MSE set to $\approx -19.5$ dB. Therefore, the step-size parameters $\mu$ of CMA and $\beta$-MMA have been chosen to obtain this steady-state performance. It can be seen that $\beta$-MMA, CNA-6 and CQA converges faster than CMA (e.g. CQA reaches its steady-state at $n=2000$ whereas that of CMA is reached at $n=7000$). We conclude from Figs. 7 and 8 that, for a fixed convergence rate, CNA with PAP achieves a lower MSE than CMA, and for a fixed steady-state performance, CNA with PAP converges faster than CMA. It is worth noting that these results are consistent with those observed in [24,23] and prove that CNA-6 and CQA are more efficient than CMA when a 16-QAM is used. Furthermore, we conclude from Fig. 8 that, for a desired steady-state performance, $\beta$-MMA, CNA-6 and CQA are equivalent methods. As a consequence, CNA-6 and CQA are potential alternatives to $\beta$-MMA.

Fig. 9 shows the performance comparison of CQA using the PAP with DR1 for $n_{PAP}$ = 250, 1000, and 4000. The CMA is plotted as reference. It can be observed that DR1 with $n_{PAP}=1000$ and 4000 have the same steady-state performance, but as expected, $n_{PAP}=1000$ converges faster than $n_{PAP}=4000$. Furthermore, Fig. 9 shows that the case DR1 with $n_{PAP}=250$ converges faster than DR1 with $n_{PAP}=1000$ but achieves higher MSE than the latter. This is due to the fact that the phase updating algorithm in (6) has

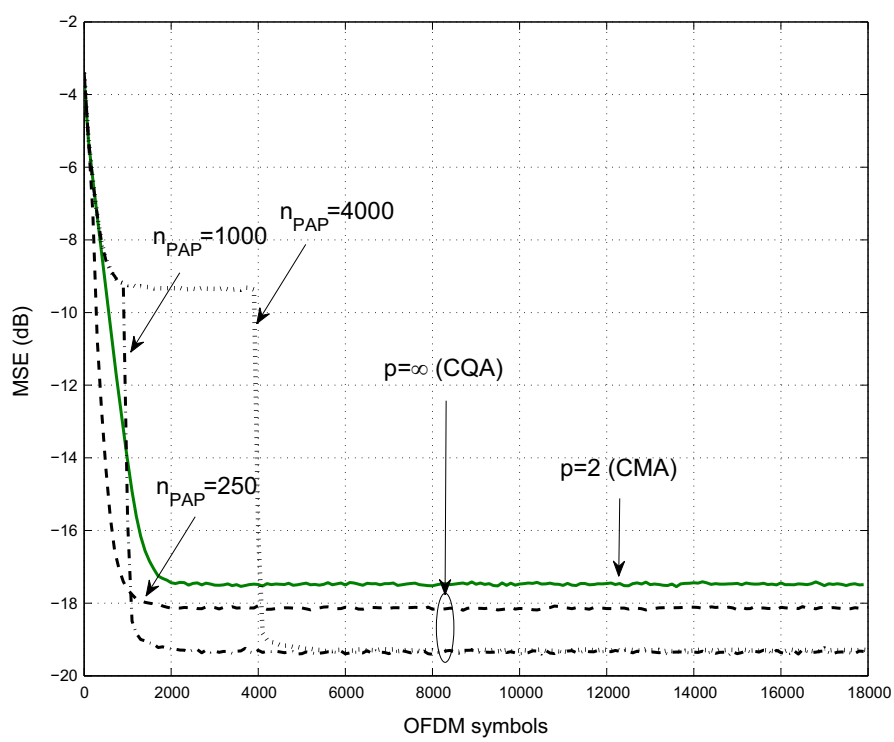


**Fig. 9.** MSE performance comparison of CQA with PAP using DR1 for $n_{PAP}$ = 250, 1000, and 4000.

freepaper.me FREE paper

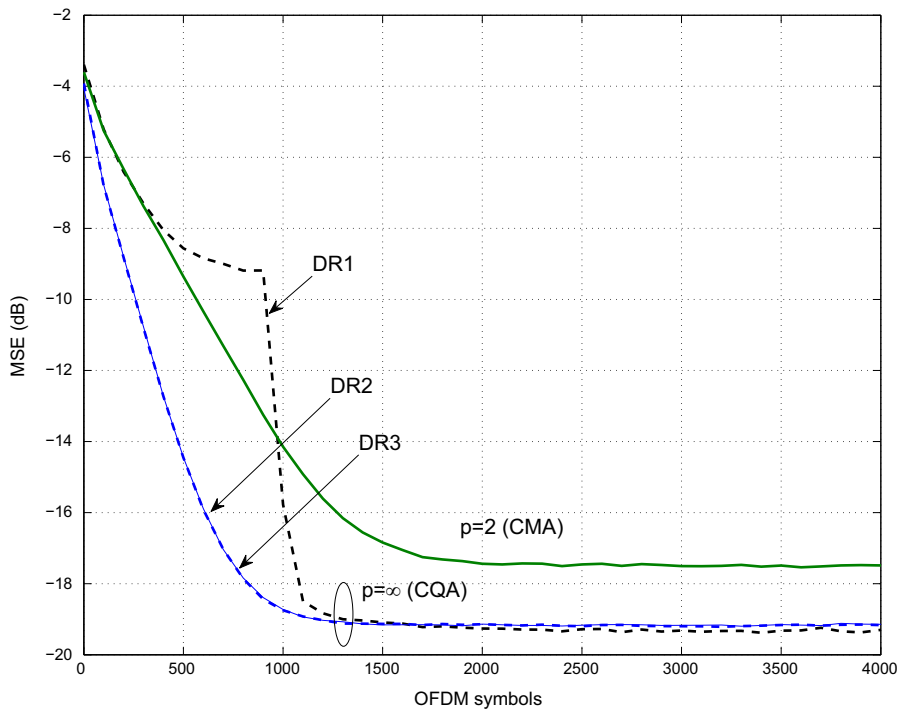


**Fig. 10.** MSE performance comparison of CQA with PAP using DR1 ($n_{PAP}$=1000), DR2, and DR3.

converged at $n_{PAP}$=250 only for a set of subcarriers (leading to a fast convergence rate), but not for the others, which induces a higher steady-state performance than the case $n_{PAP}$=1000. It results that a relevant value of $n_{PAP}$ cannot be a priori chosen, which limits the implementation of DR1.

Achieved MSEs of CQA using DR1 (with $n_{PAP}$=1000), DR2, and DR3 are compared in Fig. 10. For both DR2 and DR3, the threshold $\gamma_\phi$ has been set to 0.004, based on the recommendation made in Section 4. It can be seen that DR2 and DR3 have a higher convergence speed than DR1 and CMA (a gain of 500 iterations can be observed at MSE= − 14 dB, namely a gain of 50%), and reach almost the same steady-state performance than DR1. As a consequence, we conclude that both decision rules for the PAP can be used as a solution for the implementation of CNA in OFDM. Furthermore, it must be noticed that DR2 and DR3 have exactly the same trajectories, whereas the decision rules are different. This

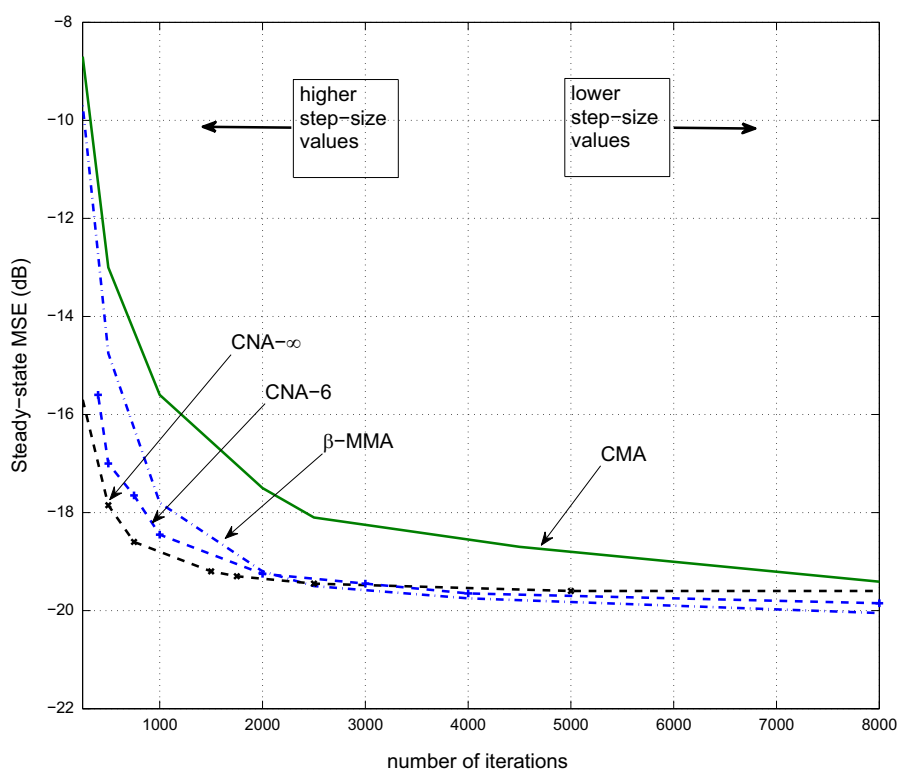


**Fig. 11.** Steady-state MSE performance versus iterations required to achieve the steady-state.

freepaper.me FREE paper

result is quite surprising, but can be explained by the fact that the MSE in (30) is averaged over 100 realizations, and for $M=128$. Therefore, it could be highlighted from Fig. 10 that DR2 and DR3 have the same performance "in average".

In order to provide a fair comparison of the performance of the different algorithms, Fig. 11 depicts the steady-state MSE performance versus iterations required to achieve the steady-state. The curves in Fig. 11 have been obtained from a set of traces corresponding to different step-size parameters values. Thus, the achieved performances in the left side of the plot correspond to high $\mu$ values (i.e. high convergence speed but low precision), whereas those on the right side of Fig. 11 correspond to lower $\mu$ values (i.e. low convergence speed but high precision). Note that both CNA-6 and CNA $-\infty$ are performed with PAP using DR2. It can be observed that in the "higher convergence speed" range (i.e. in the left side of the figure), both CNA-6 and CNA $-\infty$ outperforms $\beta$-MMA in terms of steady-state MSE. It is worth mentioning that a gain of up to 6 dB is achieved by CNA $-\infty$ compared with $\beta$-MMA where 250 iterations are required to reach the steady-state. On the other hand, $\beta$-MMA achieves a gain less than 1 dB in the "lower convergence speed" range compared with CNA-6 and CNA $-\infty$. These results reveal that CNA $-\infty$ using PAP allows us to obtain a blind equalizer combining a good convergence speed with low steady-state MSE performance.

Other simulations have been performed to analyze the behavior of CNA with PAP using DR2 when the channel changes. To be done, the same parameters as before are considered, but the coefficients of the channel are multiplied by a coefficient equal to $0.9e^{j\frac{\pi}{4}}$ at the 4000th OFDM symbol, which changes both modulus and phase. Fig. 12 shows achieved MSE performance using the CMA, CNA-6 and CQA. A peak appears in the trajectories of CNA for $p=2$, $p=6$, and $p=\infty$ at the 4000th OFDM symbol, and about 800 iterations are required by the algorithms to converge again. It can be seen that the achieved steady-state performance after the channel variation is the same as before the 4000th iteration. This result shows the capability of CNA with PAP to track the channel variations in terms of both phase and modulus.

The convergence speed of CMA and CNA-6 using the proposed sub-optimal initialization value $F_{m,n}^{s-opt}$ given in (25) is compared with the case $F_{m,n=0}=1$ in Fig. 13. It can be observed that CMA with $F_{m,n}^{s-opt}$ experiences a gain of 1000 iterations (or equivalently 1000 OFDM symbols) to reach its steady-state. Moreover, at $MSE=-16$ dB, a gain of 500 iterations is achieved by CNA-6 with $F_{m,n}^{s-opt}$ compared with $F_{m,n=0}=1$. This result validates the use of the proposed sub-optimal initialization strategy proposed Section 5 to improve the convergence speed of the CNA in OFDM systems.

### 6.3. Discussion

The previous results showed that the proposed correction of the phase mismatch allows us to adapt the CNA-6 and CQA techniques in OFDM. Moreover, these methods are able to achieve better performance in terms of MSE and convergence speed than the $\beta$-MMA [13] for high step-size parameter values. Another advantage of the CNA lies in the fact that it can be adapted to square and non-square constellations since norms can be specifically designed for all kinds of constellations. On the contrary, $\beta$-MMA is a simple method which shows good performance in the case of square constellations. Other series of simulations revealed that a blind equalizer achieves at least as good performance as pilot-aided methods. However, simulations have been undertaken in a static propagation channel. As a consequence, these blind receivers could be relevant in a broadcast context, where the channels are usually assumed to be static or quasi-static. In that scenario, a short preamble in comparison with the data sequence may not reduce that much the spectral efficiency of the data aided signal. However, the use of a preamble could increase the PAPR of the transmitted signal, whereas the PAPR of the signal using a blind receiver is that of the OFDM, i.e. about 12 dB.

## 7. Conclusion

In this paper, we have proposed an adaptation of the CNA for frequency blind equalization in OFDM. The CNA family has proved to be very relevant when a square constellation as 16-QAM is used, but has only been implemented in single carrier systems [23,24]. It

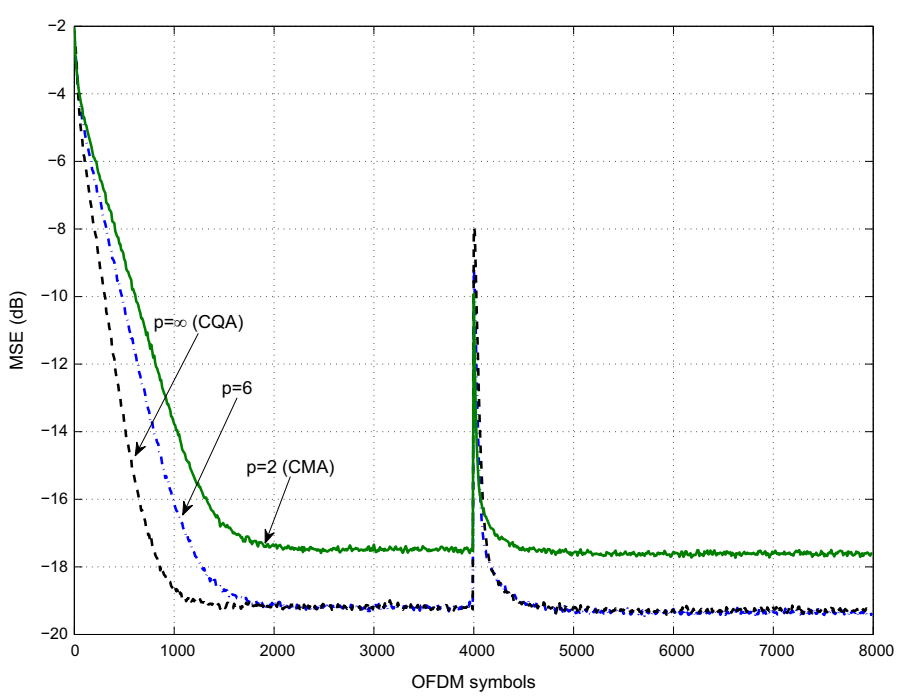


**Fig. 12.** Tracking performance of CMA, CNA-6, and CQA with PAP using DR2.

freepaper.me FREE paper

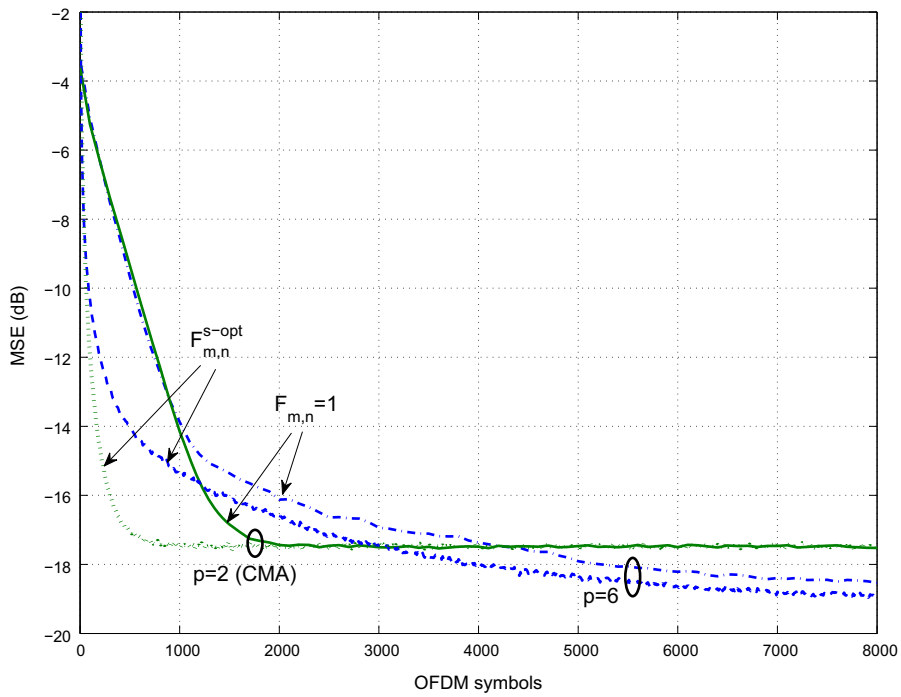


**Fig. 13.** MSE performance of CMA and CNA-6 with sub-optimal initialization strategy.

has been shown in (15) that the CNA with $p = \infty$ (CQA) is not able to recover the phase. Due to the features of CQA, this phase mismatch induces a convergence of the equalizer coefficients $F_{m,n}$ toward erroneous values, which limits the performance of this algorithm in OFDM. In order to overcome this problem, a procedure for the phase adaptation of the coefficients $F_{m,n}$ called (PAP) has been proposed in Section 4. Simulations have shown that CNA-6 and CQA with PAP outperforms the CMA, and achieves as well as $\beta$-MMA. In fact, it has been demonstrated that CNA has a higher convergence speed and achieves a lower MSE than CMA for a 16-QAM constellation. Furthermore, the capability of CNA with proposed PAP to track the channel variations has been highlighted. Finally, thanks to the proposed initialization strategy, an increase of the convergence speed is achieved.


## Acknowledgment

This work is supported by the project PROFIL (Evolution of the wideband PROfessional Mobile Radio based on the FILter Bank MultiCarrier modulation) funded by the French National Research Agency with grant agreement code ANR-13-INFR-0007-03 and ICT EC-funded project Newcom# with code FP7-IC-318306.


## Appendix A. Proof of (15)

In this appendix, we prove that the equalizer coefficients $F_{m,n+1}$ of CQA in (15) converge in average in the same direction as $F_{m,n=0}$. For sake of simplicity, a 4-QAM is considered hereafter. For any $n \in \mathbb{N}$ we rewrite $E\{\arg(F_{m,n+1})\}$ in (A.1) by substituting (12) into (15). It is assumed that $P(|\mathrm{Re}\{Z_{m,n}\}| > |\mathrm{Im}\{Z_{m,n}\}|) = P(|\mathrm{Im}\{Z_{m,n}\}| > |\mathrm{Re}\{Z_{m,n}\}|) = \frac{1}{2}$. Then, we can express $E\{\arg(A_R)\}$ as in (A.2). Since $P(Y^*_{m,n} = \pm 1 \pm j) = \frac{1}{4}$, we obtain (A.3):

$$\begin{aligned} E\{\arg(F_{m,n+1})\} &= P(|\mathrm{Re}\{Z_{m,n}\}| > |\mathrm{Im}\{Z_{m,n}\}|) \\ &\quad \times E\Big\{\arg(\underbrace{F_{m,n} - \mu(|\mathrm{Re}\{Z_{m,n}\}|^2 - R)\,\mathrm{Re}\{Z_{m,n}\}Y^*_{m,n}}_{A_R})\Big\} \\ &\quad + P(|\mathrm{Im}\{Z_{m,n}\}| > |\mathrm{Re}\{Z_{m,n}\}|) \\ &\quad \times E\Big\{\arg(\underbrace{F_{m,n} - \mu(|\mathrm{Im}\{Z_{m,n}\}|^2 - R)\,\mathrm{Im}\{Z_{m,n}\}Y^*_{m,n}}_{A_I})\Big\}. \end{aligned} \tag{A.1}$$

$$\begin{aligned} &E\{\arg(A_R)\} \\ &\quad = P(Y^*_{m,n} = 1 + j) \\ &\qquad E\Big\{\arg\Big(F_{m,n} - \mu(|\mathrm{Re}\{Z_{m,n}\}|^2 - R)\,\mathrm{Re}\{Z_{m,n}\}H_{m,n}(1 + j)\Big)\Big\} \\ &\qquad + P(Y^*_{m,n} = 1 - j) \\ &\qquad E\Big\{\arg\Big(F_{m,n} - \mu(|\mathrm{Re}\{Z_{m,n}\}|^2 - R)\,\mathrm{Re}\{Z_{m,n}\}H_{m,n}(1 - j)\Big)\Big\} \\ &\qquad + P(Y^*_{m,n} = -1 + j) \\ &\qquad E\Big\{\arg\Big(F_{m,n} - \mu(|\mathrm{Re}\{Z_{m,n}\}|^2 - R)\,\mathrm{Re}\{Z_{m,n}\} \\ &\qquad H_{m,n}(-1 + j)\Big)\Big\} + P(Y^*_{m,n} = -1 - j) \\ &\qquad E\Big\{\arg\Big(F_{m,n} - \mu(|\mathrm{Re}\{Z_{m,n}\}|^2 - R)\,\mathrm{Re}\{Z_{m,n}\} \\ &\qquad H_{m,n}(-1 - j)\Big)\Big\}. \end{aligned} \tag{A.2}$$

$$\begin{aligned} &E\{\arg(A_R)\} \\ &\quad = \tfrac{1}{4}E\Big\{\arg\Big(F_{m,n} - \mu(|\mathrm{Re}\{Z_{m,n}\}|^2 - R)\,\mathrm{Re}\{Z_{m,n}\}H_{m,n}(1 + j)\Big) \\ &\qquad + \arg\Big(F_{m,n} - \mu(|\mathrm{Re}\{Z_{m,n}\}|^2 - R)\,\mathrm{Re}\{Z_{m,n}\}H_{m,n}(1 - j)\Big) \\ &\qquad + \arg\Big(F_{m,n} - \mu(|\mathrm{Re}\{Z_{m,n}\}|^2 - R)\,\mathrm{Re}\{Z_{m,n}\}H_{m,n}(-1 + j)\Big) \\ &\qquad + \arg\Big(F_{m,n} - \mu(|\mathrm{Re}\{Z_{m,n}\}|^2 - R)\,\mathrm{Re}\{Z_{m,n}\}H_{m,n}(-1 - j)\Big)\Big\} \end{aligned} \tag{A.3}$$

freepaper.me FREE paper دانلود کننده مقالات علمی

It is straightforward to show that for any $(z_1, z_2) \in \mathbb{C}^2$, we have

$$\arg\left(z_1 + z_2 e^{j\frac{\pi}{4}}\right) + \arg\left(z_1 + z_2 e^{j\frac{3\pi}{4}}\right) + \arg\left(z_1 + z_2 e^{-j\frac{\pi}{4}}\right) + \arg\left(z_1 + z_2 e^{-j\frac{3\pi}{4}}\right) = 4\arg(z_1). \tag{A.4}$$

Then, by substituting the result in (A.4) into (A.3), we obtain that $E\{\arg(A_R)\} = \arg(F_{m,n})$. The same development can be carried out with $E\{\arg(A_I)\}$ leading to the equality $E\{\arg(F_{m,n+1})\} = E\{\arg(F_{m,n})\}$ in (A.1). As this result is valid for any $n \in \mathbb{N}$, a simple mathematical induction yields

$$E\{\arg(F_{m,n+1})\} = E\{\arg(F_{m,n=0})\}. \tag{A.5}$$

### A.1. Proof of (22)

The substitution of (21) into (20) yields

$$\begin{aligned}\gamma_\phi &= \mu_\phi^2 E\{\mathrm{Im}\{\tilde{Z}_{m,n}\tilde{W}_{m,n}^*\}^2\} = \mu_\phi^2 E\{\mathrm{Im}\{a_{m,n}\tilde{W}_{m,n}^* + |\tilde{W}_{m,n}|^2\}^2\} \\ &= \mu_\phi^2 E\left\{\left(\mathrm{Im}\{a_{m,n}\}\,\mathrm{Re}\{\tilde{W}_{m,n}^*\} + \mathrm{Re}\{a_{m,n}\}\,\mathrm{Im}\{\tilde{W}_{m,n}^*\}\right)^2\right\}.\end{aligned} \tag{A.6}$$

The expectation of the cross-factors obtained from the development of the third line in (A.6) are equal to zero since both $a_{m,n}$ and $\tilde{W}_{m,n}$ are variables with zero mean. Hence, using $\tilde{\sigma}^2 \geq \sigma^2$ leads to the following:

$$\begin{aligned}\gamma_\phi &= \mu_\phi^2 E\{\mathrm{Im}\{a_{m,n}\}^2\,\mathrm{Re}\{\tilde{W}_{m,n}^*\}^2 + \mathrm{Re}\{a_{m,n}\}^2\,\mathrm{Im}\{\tilde{W}_{m,n}^*\}^2\} \\ &\geq \mu_\phi^2 \tilde{\sigma}^2 E\{\mathrm{Re}\{a_{m,n}\}^2 + \mathrm{Im}\{a_{m,n}\}^2\} \\ &\geq \mu_\phi^2 \sigma^2 E\{\mathrm{Re}\{a_{m,n}\}^2 + \mathrm{Im}\{a_{m,n}\}^2\}.\end{aligned} \tag{A.7}$$

Note that the covariance of $\mathrm{Im}\{a_{m,n}\}^2$ and $\mathrm{Re}\{\tilde{W}_{m,n}^*\}^2$ has been omitted in the second line of (A.7), which justify the use of the inequality.

## References


[1] M. Morelli, U. Mengali, A comparison of pilot-aided channel estimation methods for OFDM systems, IEEE Trans. Signal Process. 49 (12) (2001) 3065–3073.
[2] M.K. Ozdemir, H. Arslan, Channel estimation for wireless OFDM systems, IEEE Commun. Surv. Tutor. 9 (2) (2007) 18–48.
[3] Y. Liu, Z. Tan, H. Hu, L.J. Cimini, G.Y. Li, Channel estimation for OFDM, IEEE Commun. Surv. Tutor. 16 (4) (2014) 1891–1908.
[4] Y. Sato, A method of self-recovering equalization for multilevel amplitude-modulation systems, IEEE Trans. Commun. 23 (6) (1975) 679–682.
[5] D.N. Godard, Self-recovering equalization and carrier tracking in two-dimensional data communication systems, IEEE Trans. Commun. 28 (11) (1980) 1867–1875.
[6] J. Treichler, B. Agee, A new approach to multipath correction of constant modulus signals, IEEE Trans. Acoust. Speech Signal Process. 31 (2) (1983) 459–472.
[7] R. Johnson, Jr., P. Schniter, T. Endres, J. Behm, D. Brown, R. Casas, Blind equalization using the constant modulus criterion: a review, Proc. IEEE 86 (10) (1998) 1927–1950.
[8] J. Yang, J.-J. Werner, Dumont, G.A. The multimodulus blind equalization and its generalized algorithms, IEEE Trans. Sel. Areas Commun. 20 (5) (2002) 997–1015.
[9] K. Wesolowski, Analysis and properties of the modified constant modulus algorithm for blind equalization, Eur. Trans. Telecommun. 3 (1992) 225–230.
[10] K.N. Oh, Y.O. Chin, Modified constant modulus algorithm: blind equalization and carrier phase recovery algorithm, in: ICC'95, vol. 1, Seattle, WA, 1995, pp. 498–502.
[11] S. Abrar, A.K. Nandi, Blind equalization of square-QAM signals: a multi-modulus approach, IEEE Trans. Commun. 58 (6) (2010) 1674–1685.
[12] J. Mendes Filho, M.D. Miranda, M.T.M. Silva, A regional multimodulus algorithm for blind equalization of QAM signals: introduction and steady-state analysis, Signal Process. 92 (11) (2012) 2643–2656.
[13] S. Abrar, A.K. Nandi, Adaptive solution for blind equalization and carrier-phase recovery of square-QAM, IEEE Signal Process. Lett. 17 (9) (2010) 791–794.
[14] A.W. Azim, S. Abrar, A. Zerguine, A.K. Nandi, Steady-state performance of multimodulus blind equalizers, Signal Process. 108 (2015) (2015) 509–520.
[15] T.C. Hewavithana, D.M. Brookes, Blind adaptive channel equalization for OFDM using the cyclic prefix data, in: GLOBECOM'04, vol. 4, 2004, pp. 2376–2380.
[16] M. de Courville, P. Duhamel, P. Madec, J. Palicot, Blind equalization of OFDM systems based on the minimization of a quadratic criterion, in: ICC'96, vol. 3, Dallas, TX, 1996, pp. 1318–1322.
[17] H. Zamiri-Jafarian, H. Khoshbin, S. Pasupathy, Time-domain equalizer for OFDM systems based on SINR maximization, IEEE Trans. Commun. 53 (6) (2005) 924–929.
[18] M. Luise, R. Reggiannini, G. Vitetta, Blind equalization/detection for OFDM signals over frequency-selective channels, IEEE Trans. Sel. Areas Commun. 16 (8) (1998) 1568–1578.
[19] T. Al-Naffouri, A. Dahman, M. Sohail, W. Xu, B. Hassibi, Low-complexity blind equalization for OFDM systems with general constellations, IEEE Trans. Signal Process. 60 (12) (2012) 6395–6407.
[20] K. Van Acker, G. Leus, M. Moonen, O. Van de Viel, T. Pollet, Per tone equalization for DMT-based systems, IEEE Trans. Commun. 49 (1) (2001) 109–119.
[21] R.K. Martin, Blind, adaptive equalization for multicarrier receivers (Ph.D. thesis), Cornell University, Ithaca, NY, 2004.
[22] B.H.B. Naeeni, H. Amindavar, H. Bakhshi, Blind per tone equalization of multilevel signals using support vector machines for OFDM in wireless communication, Int. J. Electron. Commun. 64 (2) (2010) 186–190.
[23] A. Goupil, J. Palicot, Constant norm algorithms class, in: Proceedings of EUSIPCO'02, Toulouse, France, 2002.
[24] A. Goupil, J. Palicot, New algorithms for blind equalization: the constant norm algorithm family, IEEE Trans. Signal Process. 55 (4) (2007) 1436–1444.
[25] T. Thaiupathump, New algorithms for blind equalization and blind source separation/phase recovery (Ph.D. thesis), University of Pennsylvania, Philadelphia, PA, January 2002.
[26] T. Thaiupathump, L. He, S.A. Kassam, Square contour algorithm for blind equalization of QAM signals, Signal Process. 86 (11) (2006) 3357–3370.
[27] N. Benvenuto, G. Cherubini, Algorithms for Communications Systems and their Applications, Wiley, Chichester, England, 2002.
[28] V. Savaux, Contribution to multipath channel estimation in OFDM context (Ph. D. thesis), Supélec, Rennes, France, November 2013.
[29] G. Picchi, G. Prati, blind equalization and carrier recovery using a "stop-and-go" decision-directed algorithm, IEEE Trans. Commun. 35 (9) (1987) 877–887.
[30] A. Belouchrani, W. Ren, Blind carrier phase tracking with guaranteed global convergence, IEEE Trans. Signal Process. 45 (7) (1997) 1889–1894.
[31] Y. Ha, W. Chung, Non-data-aided phase noise suppression scheme for CO-OFDM systems, IEEE Photon. Technol. Lett. 25 (17) (2013) 1703–1706.
[32] J.G. Proakis, Communication through band-limited channels, in: Digital Communications, Mc Graw-Hill, New York, 1995, pp. 583–635 (Chapter 10).


دانلود کننده مقالات علمی freepaper.me FREE paper